Supplementary Material

Effect of threading on Static and Dynamic Properties of Polymer Chains in Entangled Linear-Ring Blend Systems with Different Stiffness

Wei Wang,[b] Jibao Lu,[a,b]* Rong Sun,[a,b]

[a] Shenzhen Institute of Advanced Technology, Chinese Academy of Sciences, Shenzhen 518055, China.

[b] Shenzhen Institute of Advanced Electronic Materials, Chinese Academy of Sciences, Shenzhen 518055, China.

* Corresponding author.

E-mail addresses: jibao.lu@siat.ac.cn (Jibao Lu)

S1. Reduction of piercing points

In our protocol, all LP chains are separated by the piercing point, and the adjacent piercing points separated by a sub-chain with a length smaller than the cutoff length are reduced (See Figure S1(a)). After merging the piercing points, the sub-chain lengths are checked again. Those shorter than the cutoff length are considered as transient piercing and then removed, the remaining piercing points are taken as effective threading points. The resulting threading number of RPs obtained in this way are re-examined using PPA methods (Figure S1(b)). To obtain the primitive path, two ends of LP chains are fixed and intramolecular interactions are turned off, while the intermolecular LJ and bonded interactions remain the same. The systems are then allowed to relax freely at a low temperature, then all chains shrink into their primitive path.[1] Consistent results can be obtained with the two methods. Using this strategy, the threading number of RP chains can be obtained directly without closing the LP chains.[1, 2]

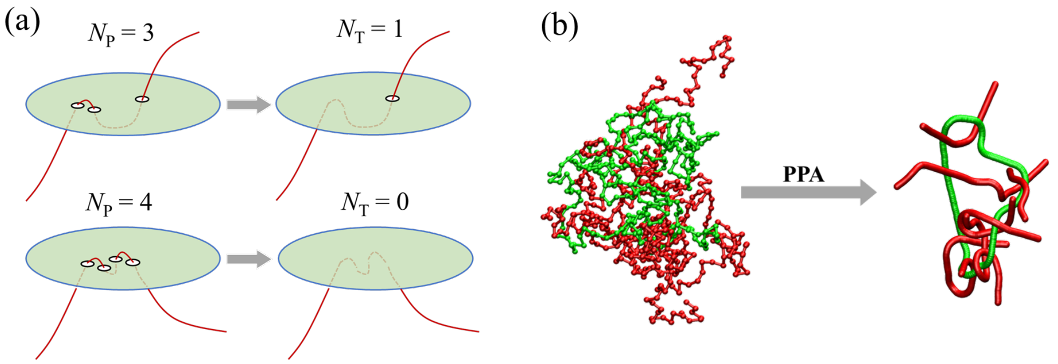

Figure S1. (a) Schematic view of the piercing point reduced technique. (b) Configures reexamined using PPA method, LP chains and the threaded RP chain are colored in red and green respectively.

The piercing number obtained directly from the above method is denoted as N_P. By using the IMS technique, both N_P and effective threading number N_T are obtained. Since not every piercing can be taken as an effective threading, so the ratio of N_P and N_T will always be greater than 1. We plot N_P against the entanglement number of RP chains in Fig. S2. From Fig. S2, we find that N_P is systematically larger for much more flexible chains. Meanwhile, N_P of k_θ = 1.5 and 2.0 are very similar for the systems with RP chains with approximately the same entanglement number, indicating that the threading events tend to be stable when the stiffness of the system increases to a certain level. Interestingly, we also find that the relationship $N_P \sim Z_R^\gamma$ holds for all systems. The value of γ is 1.352, 1.290 and 1.289 for the cases k_θ = 0.75, 1.5, and 2.0 separately. We can see the exponent value is also close for k_θ = 1.5 and 2.0.

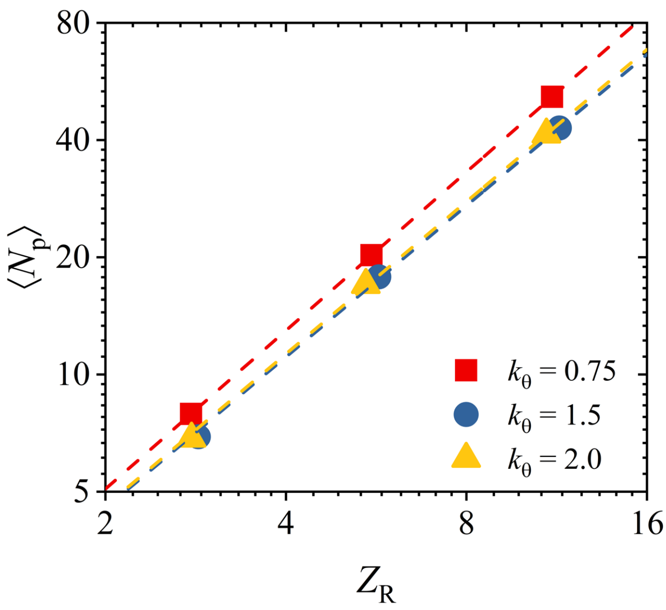

Figure S2. The average piercing number $\langle N_P \rangle$ for RP chains versus the entanglement number of RP chains Z_R. Dashed lines are fitting curves of the equation $\langle N_P \rangle = cZ_R^{\gamma}$.

S2. Mutual effects between LP and RP

Compared to the conventional entanglement, which is determined between two LP chains, thread can be considered as an entanglement formed between LP and RP chains. In pure LP melt with entanglement number Z_L, there will be Z_L entanglements are formed between the central LP with other chains in the system. While in LRB with LP fraction ϕ, the possibility it entangles with RP chain is (1-ϕ), so on average there should be $\langle N_T \rangle_L = Z_L(1-\phi)$ entanglements formed between LP chain and RP chain. For our LRB systems with Z_L=6, the value of $\langle N_T \rangle_L$ is summarized in Fig. S3(a), and little dependence of $\langle N_T \rangle_L$ on Z_R is found, implying that for all entanglements of a central LP chain, the contribution of RP is a relatively constant value. Here we define the upper bound as $(Z_{L,max}+1)(1-\phi)$, and the lower bound as $(Z_{L,min}+1)(1-\phi)$, where $Z_{L,max}$ = 5.71 and $Z_{L,min}$ = 5.56 are the maximum and minimum values of the entanglement number of the LP chain as defined in **Section 2.1** of the main text. The region between the two boundaries is shaded in green in Fig. S3(a). We find that our theoretical prediction underestimates the real value of $\langle N_T \rangle_L$, and as the chain stiffness increases, the discrepancy becomes more pronounced. As we have discussed earlier, the threading number of RP chains is larger for stiffer LRB systems, so it is not surprising that, on average, more RP chains found threaded along each LP chain at the same entanglement level.

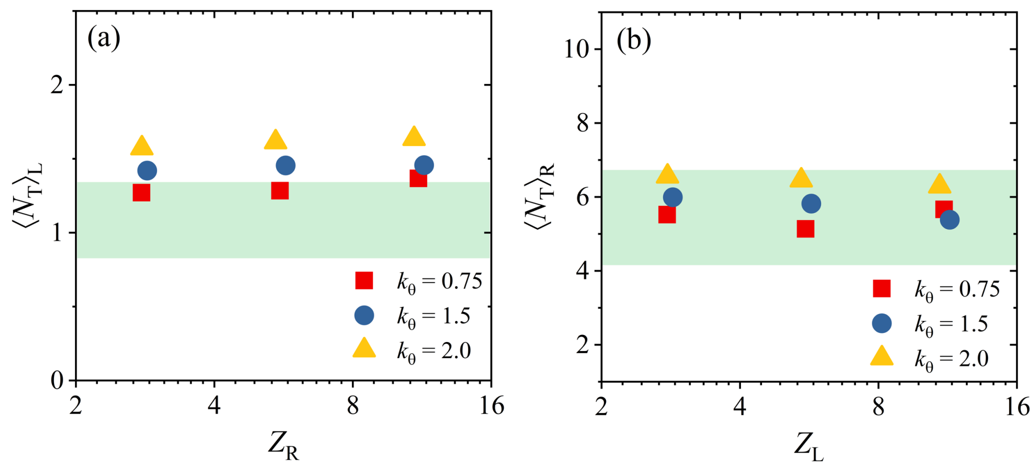

Figure S3. (a) $\langle N_T \rangle_L$ plotted versus Z_R in LRB with fixed Z_L=6. (b) $\langle N_T \rangle_R$ plotted versus Z_L in LRB with fixed Z_R=6. The shaded region is explained in the main text.

On the other hand, we are also interested in whether the threading number of the RP chain varies when mixed with LP chains of different chain lengths. Therefore, we turn to LRB systems with fixed Z_R=6 and varying Z_L. The average threading numbers for RPs (denoted as $\langle N_T \rangle_R$) are plotted against the entanglement number of LP chains Z_L (Fig. S3(b)). And we find that $\langle N_T \rangle_R$ is irrelevant with Z_L, which means that the threading number is an intrinsic property for RPs in LRB with a fixed fraction of LP as the main component, and it cannot be tuned by changing the chain length of LP components. Meanwhile, we find that the values of $\langle N_T \rangle_R$ for all systems are closed to the predetermined entanglement value Z_R. Similarly, we also define a region with the upper and lower bounds equals to $Z_{R,max}$+1 and $Z_{R,min}$-1, where $Z_{R,max}$ = 5.71 and $Z_{R,min}$ =5.56 are the maximum and minimum values of RP chain for the three stiffness. Region between the two bounds is shaded in green in Figure S3(a). We can see that all the values basically fall within the region. This fact again confirms that threading number of RP chains can be approximated by their entanglement number, regardless of the chain length of the LP chain in LRB, as long as LP is the dominant component.

In the previous section, we have found that $\langle N_T \rangle_L$ does not change with Z_R, and vice versa. Furthermore, we wonder whether the static properties of LP/RP chains are affected by increasing/decreasing the chain length of the other component. The $\langle R_g^2 \rangle$ of LP with fixed Z_L = 6 is summarized versus Z_R in Fig. S4(a), and we find that the size of LP chains with various stiffness does not change by blending with RP chains, regardless the chain length of RP chains. This means that the size of LP chains in our LRB system is not changed by mixing RP chains. To compare with the size of LP chain in the pure melt state, we also summarized the normalized $\langle R_g^2 \rangle$ in Table S1. It is clear that there is no difference in size between the LP chains in LRB and in pure melt. This is partly due to the small fraction of RP chains (20%), the amount of which is not large enough to induce discernible differences with pure LP melts. Meanwhile, since the RP chains are fully penetrated, they behave as if they were LP chains in LRB. This makes it much easier to predict the properties of LRB, since the properties of LP chains in LRB is expected to be the same as those of pure LP melts.

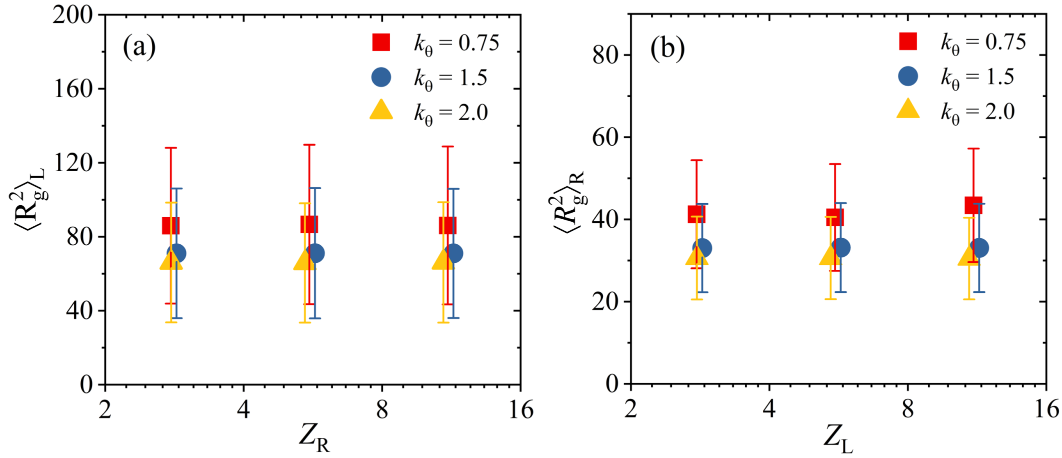

Figure S4. (a) $\langle R_g^2 \rangle_L$ versus Z_R in LRB with fixed Z_L=6 and (b) $\langle R_g^2 \rangle_R$ versus Z_L in LRB with fixed Z_R=6.

We then we turn to LRB with Z_R=6 and varying Z_L. The $\langle R_g^2 \rangle$ of RP chains are plotted against Z_L in Fig. S4(b), and we find that the size of RP chains is also irrelevant to the chain length of LP chains. We also summarize the value of the normalized $\langle R_g^2 \rangle$ of RP chains in Table S1. Here we find a universal swelling ratio for RP of about 1.30±0.025, regardless of the length of the LP chains. This fact again suggests the same threading ability of LP chains to RP chains of different chain length when the LP component dominates in LRB.

Table S1. Normalized $\langle R_g^2 \rangle$ of LP/RP chains in LRB with fixed LP/RP chain length

k_θ	$\langle R_g^2 \rangle_L / \langle R_g^2 \rangle_{L,0}$			$\langle R_g^2 \rangle_R / \langle R_g^2 \rangle_{R,0}$		
	$Z_R = 3$	$Z_R = 6$	$Z_R = 11$	$Z_L = 3$	$Z_L = 6$	$Z_L = 11$
0.75	0.993	1.000	0.994	1.290	1.266	1.358
1.5	1.000	1.001	0.997	1.288	1.293	1.290
2.0	0.994	0.999	1.001	1.297	1.297	1.292

S3. Dynamic properties

The value of the characteristic time τ_1 and τ_2 are summarized in Table S2. τ_1 and τ_2 are defined as the time when the fitting curve of correlation function $\chi(t)$ is equal to 0.4 and 0.2 separately using equation (8) of the main text.

Table S2. Summary of τ_1 and τ_2

k_θ	τ (χ = 0.4) /$10^5\tau$			τ (χ = 0.2) /$10^5\tau$		
	Z_R = 3	Z_R = 6	Z_R = 11	Z_R = 3	Z_R = 6	Z_R = 11
0.75	1.79	1.66	2.19	8.46	8.55	13.0
1.5	1.09	1.03	1.20	3.94	4.44	5.96
2.0	0.836	0.816	0.931	2.66	3.10	4.05

References

1. Hagita, K.; Murashima, T. Effect of chain-penetration on ring shape for mixtures of rings and linear polymers. *Polymer* **2021,** 218,

2. Hagita, K.; Murashima, T. Molecular Dynamics Simulations of Ring Shapes on a Ring Fraction in Ring–Linear Polymer Blends. *Macromolecules* **2021,** 54 (17), 8043-8051

3. Smrek, J.; Grosberg, A. Y. Minimal Surfaces on Unconcatenated Polymer Rings in Melt. *ACS Macro Letters* **2016,** 5 (6), 750-754

4. Smrek, J.; Kremer, K.; Rosa, A. Threading of Unconcatenated Ring Polymers at High Concentrations: Double-Folded vs Time-Equilibrated Structures. *ACS Macro Lett* **2019,** 8 (2), 155-160